

TERRESTRIAL INVERTED CHANNELS IN UTAH: ANALOGS FOR INVESTIGATION OF MARTIAN SINOUS RIDGES. R. M. E. Williams¹, ¹Planetary Science Institute, 1700 E. Fort Lowell, Suite 106, Tucson, AZ 85719, williams@psi.edu.

Overview: Many sinuous ridge landforms on Mars have branching planimetric patterns similar to terrestrial rivers and continuity relationships with Martian valley networks. These attributes support the interpretation that these landforms are water carved drainage networks now preserved in inverted relief [1]. In order to accurately interpret the Martian fluvial history preserved in these landforms, a better understanding based on terrestrial analogs is needed. Multiple examples of inverted paleochannels are present within the state of Utah. This report will describe two sites: lava-capped paleochannels near St. George and exhumed, cemented paleochannels of the Cedar Mountain Formation (CMF) located southwest of Green River. Evaluation of paleohydrologic models for the CMF paleochannels demonstrates the applicability of empirically and theoretically-derived models from modern terrestrial streams to inverted channels. Application of these models to Martian sinuous ridges will yield additional insight into the amount of water and duration of fluvial activity at various locations. This information, combined with the geologic setting and morphology, is fundamental to assessing how the fluvial environment and flow conditions changed with time and/or geographic location.

Sinuous Ridges on Mars: Martian sinuous ridges range in size, but are commonly tens to a few hundred meters wide and hundreds to thousands of meters in length. Although most sinuous ridges are smaller than typical valley networks (few kilometers width, 20-200 km long; [2,3]), there are several examples of valley networks that are laterally traceable to positive-relief sinuous ridges [e.g. 1]. Sinuous ridges exhibit a variety of planimetric patterns ranging from single, curvilinear ridge forms to branching networks.

Interpretations for sinuous ridges have varied. Many researchers have invoked running water in their formation but differ in the source of the water: 1) precipitation-fed surface runoff created former fluvial channels formed by continually flowing water, now expressed in inverted relief due to differential erosion [1,4-6], and 2) meltwater generated within, beneath or adjacent to a glacier [e.g. 7-11] or derived from impact into a volatile-rich substrate [12].

In addition to these hypotheses, nonfluvial formation mechanisms have been proposed for sinuous ridges in select cases, such as the large-scale sinuous ridges in Argyre Planitia (10-200 km long, 1-4 km

wide; [10]). Proposed interpretations include wrinkle ridges, exhumed igneous and clastic dikes, lava flows features, and linear sand dunes [see references in 10]. It is the continuity relationship of sinuous ridges with valley networks and their planimetric pattern (e.g. branching networks, meandering) that suggest most sinuous ridges are former fluvial channels now preserved as inverted landforms.

A catalog of sinuous ridge locations has been compiled by the author based primarily on nonsystematic MOC, THEMIS and CTX image review. Presently, there are ~250 sinuous ridge systems within the catalog, which continues to expand based on new data. The spatial distribution and geologic setting of sinuous ridges differs from that of valley networks. While both landforms are predominantly located on the cratered uplands, valley networks are preferentially located at surface elevations >2 km [2] and sinuous ridges are found at a range of elevations, including many examples that are located on terrain below the 0 m Martian datum [5]. Unlike valley networks, several sinuous ridges have been identified on crater floors. There are regional clusters of these landforms including on the plains proximal to Valles Marineris and nearby chasmata, along the dichotomy boundary in the eastern hemisphere notably associated with the Aeolis/Zephyria Plana region [11], in northwest Arabia Terra and along the northern rim of Hellas basin [5].

Osterloo identified chloride-bearing materials, potentially chloride salts that formed via evaporation, in THEMIS daytime infrared images (100 m/pix) and a few of these locations were associated with sinuous channels [13]. Preliminary analysis of an updated catalog of 635 chloride locations (Osterloo, pers. comm.) indicates that the vast majority of Martian sinuous ridges do not correspond to the same locations, although the scale of many sinuous ridges may be below THEMIS resolution.

Rudimentary ages can be assigned to valley networks and sinuous ridges based on cross-cutting and superposition relationships, respectively, with mapped geologic units [14,15]. Thus, this method yields formation ages for valley networks and maximum ages for sinuous ridges. Some sinuous ridges may have undergone burial and exhumation, processes which can complicate age assessments from crater statistics. Although this approach is problematic [16], comparison using the same approach employed in prior stu-

dies yields an interesting difference in apparent ages for these landforms (Table 1).

Carr [2], expanded by Hynek et al. [17], both determined that the vast majority of valley networks have a maximum age of Noachian. Williams [5] looked at a smaller sample size of sinuous ridges and found equal numbers in the Noachian and post-Noachian time periods. Assuming the age assessments are valid, the youngest sinuous ridges are generally not associated with high slopes or volcanoes (presumably sites of high geothermal gradients), as was observed for Amazonian-aged valley networks [2].

The drainage density (stream length per unit area, D_d), of valley networks is a few orders of magnitude less than terrestrial river systems, perhaps due in part to differences in mapping scale [2,17]. However, some sinuous ridges have drainage densities an order of magnitude higher than has been observed for valley networks [5]. These values coincide with the lower range of observed terrestrial fluvial systems at the same scale. The space-filling distribution of some sinuous ridge networks is additional evidence in support of overland flow in producing these landforms.

Table 1

	Valley Networks		Sinuous ridges
	Carr (1995) [2]	Hynek et al. (2008) [17]	Williams (2007) [5]
Total #	827	~2900 ¹	175
Max. D_d (km^{-1})	0.02	0.14	2.3 ²
Noachian	90%	84%	51%
Hesperian	5%	10%	31%
Amazonian	5%	6%	18%

¹Number of valley segments, not networks, which likely reflect a slight increase in number of valley networks, but no more than a factor of two from Carr's [2] assessment (Hynek, pers. comm.)

²Williams et al., 2005 [1].

Recent review of THEMIS VIS images have identified ~150 sinuous ridge sections in the Aeolis/Zephyria Plana region [11], which are presumed to be Amazonian in age but were not wholly accounted for in the Williams 2007 study. Further investigation of this site will determine the number of individual systems as the discontinuous VIS coverage did not permit continuity relationships between segments to be assessed. However, these preliminary results suggest that the number of post-Noachian sinuous ridges has been under-represented in the Williams [5] study.

Martian valley systems, as observed today, are the products of the combined forces of burial, exhumation and erosion. Thus, sinuous ridges expand the preserved record of fluvial activity on Mars. The sinuous ridges are observed on several terrains that have been

mapped as heavily eroded or degraded regions including the Aeolis/Zephyria Plana region and northwestern Arabia Terra [18,19]. These locations are windows into the Martian stratigraphy and provide a more complete temporal record of fluvial activity.

Altogether, these observations suggest that fluvial activity was more prevalent in the post-Noachian time period than previously recognized. Small-scale fluvial activity appears to have occurred periodically, at least in locations, throughout Martian history. Further study of these landforms has the unique potential to assess temporal changes in fluvial style on Mars. The investigation of inverted fluvial systems on Earth is useful for recognizing diagnostic attributes of inverted paleochannels both in terms of induration agent (i.e. lava-capped versus cemented) and to distinguish these landforms from other hypothesized formation mechanisms. Additionally, field observations enable the evaluation of hydrologic models for terrestrial inverted paleochannels.

Field Sites

St. George vicinity, Utah Lava flows originate at cinder cones located at the base of the Pine Valley Mountains and flowed several miles down ancient drainage pathways of the Virgin River [20]. These cinder cones formed at various elevations due to regional uplift and were intermittently active over the past few million years. The lava-capped channels blocked drainage creating lakes and alternate flow pathways. Commonly, parallel drainage developed on either side of the lava flow. Over time erosion at the lateral margin of the lava flow results in a sinuous ridge. The inverted valley was further degraded into a series of mesas and buttes present today.

Southwest of Green River, Utah The longest (spanning ~12 km) known inverted paleochannel system on the Colorado Plateau consists of four conglomeratic/sandstone-capped ridges, some with bifurcations along route, and numerous shorter ridges segments within the Ruby Ranch Member of the Cedar Mountain Formation. Harris [21] mapped the site, located 11 km southwest of Green River, and found individual inverted paleochannel segments with lengths that range from 4.5 to 8 km. The inverted channels stand 30 to 40 m above the surrounding plains. Multiple stages of paleochannel activity are preserved here and channels were not all formed contemporaneously. These single-thread channels are generally linear, although some sections exhibit low sinuosity with sinuosity ratios between 1.2 and 1.5 [21]. Fluvial activity within these channels may not have been contemporaneous as two of the exhumed channels exhibit a clear superposition relationship. Channel preservation is discontinuous; where the cap-

stone has been removed, the underlying mudstone erodes to a rounded cross-sectional shape.

The streams flowed in a strongly seasonal, semiarid climate. Groundwater flows more easily through the porous channel deposits than through the mud overbank deposits. Evaporation of groundwater concentrated calcium carbonate and other minerals at the surface during the dry season, indurating the fluvial deposits [21]. In addition to carbonate cement, Lorenz et al. [22] reported localized quartz cement, both grain-coating and pore-filling, binding the fluvial sediments. These fluvial sediments were first buried by marine sediments from a Late Cretaceous inland sea. Burial history models for the region indicate that ultimately 2400 meters of sediment overburden was laid down in various depositional environments [23,24]. Following burial, the region underwent uplift and exhumation in middle to late Cenozoic time. The encasing softer floodplain mudstone was eroded away by fluvial denudation, and the ancient fluvial deposits are now preserved as elongated ridges. Based on long-term erosion rates for the region (0.06 m/kyr; [23,24]) and present day surface relief, the maximum surface re-exposure age for the fluvial sediments at this site is 650,000 years [25].

Exhumed paleochannel surfaces at this site preserve both sand-sized channel-fill deposits and gravel-rich point-bar deposits concentrated on the inside inflections of channel bends. The caprock (up to 10 m thick) preserves an aggrading channel bed, and the strata exposed at the surface represents deposits from more than one flow event. Cross-bed sets in the sandstones are expressed both in vertical exposures and on the ridge surfaces, in the latter case as scalloped textures that are broadly concave in the downstream (east and north) direction. Weathering of point-bar deposits produces an irregular surface, non-vertical walls, and variable channel widths, whereas channel-fill deposits erode into a relatively smooth surface and vertical cliffs with better preservation of the original channel width [21,26].

Cemented paleochannel deposits, now exposed as ridge-forms due to landscape inversion, preserve key attributes of the former fluvial environment. A record of the fluvial conditions during active flow such as original channel shape (preserved in some sections), flow direction, and sediment transport capability is preserved. Paleochannel dimensions, slope, and grain size distribution can be used to estimate paleoflow conditions with paleohydraulic models.

Paleohydrologic Models Two approaches to paleodischarge estimation were employed to produce an envelope of discharge estimates based on several dif-

ferent models. This method enables an exploration of parameter space and will help to mitigate many of the limitations and errors in both model assumptions and field measurements. Examining this suite of models for terrestrial analogs provides ground truth and reassurance in applying these models to Martian inverted channel systems, where additional assumptions are necessary due to the reliance on remotely sensed data. These models were assessed for the CMF cemented paleochannels; future phases of this research will evaluate the applicability of these models to other inverted paleochannels including lava-capped examples.

All of the methods of paleoflow determination are based on direct analogies either with hydraulic relations between sediment and flow parameters in present-day streams or flumes, or with geomorphic relations between channel morphology, channel sediments, and discharge measures observed in modern rivers. The hydraulic or micro-approach [e.g. 27], provides estimates of short-term (or instantaneous) velocity or discharge conditions, as a result of local adjustment of hydraulic geometry around a mean or equilibrium channel condition. The geomorphic or macro-approach indicates the development of longer-term equilibrium or quasi-equilibrium conditions between catchment, channel, and flow parameters [e.g. 28]. Full details of the models employed in this study are described in [26].

Field based measurements, including Differential Global Positioning System (DGPS) topographic surveys and clast size distribution characterization for two inverted paleochannel segments at the site were used as input parameters in the paleohydrologic models. Slope magnitude was corrected for the slight regional structural dip (e.g. [22]), assuming perfect original horizontality, to obtain an estimate of the paleochannel slope. At critical flow velocities were between 1.5 and 2.5 m/s, and discharges ranged from 150 to 493 m³/s. Derived values are consistent with field observations that constrain flow conditions and depth [26]. The macro-approach yielded discharge values that were generally slightly higher than those derived from the micro-approach and the resulting mean discharge value tended toward the extreme of the range obtained from either method (Figure 1). The range of discharge values determined from the micro-approach overlaps the field of values determined from the macro-approach, showing consistency in results from two different methodologies. The equations applied in this analysis represent a range of fluvial environments, and a much more confined range of plausible discharge values can be identified by selecting those relationships formulated for a given fluvial environment (a gravel-bedded stream, in this

case). However, in the absence of such knowledge, it is noteworthy that the overall range of discharge values obtained from all methods employed is within one order of magnitude.

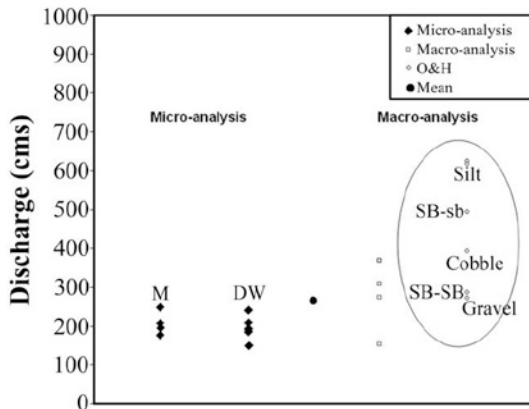


Figure 1: Computed discharges from multiple models (see [26] for details) for a CMF inverted paleochannel are plotted with arbitrary offset on the x-axis for clarity. Discharge values obtained from [29], enclosed in oval and not included in computation of mean, illustrate the effect of bed material size on discharge. Discharges obtained from relations for the coarser bed material agree well with discharge obtained from other methods in this study. Abbreviations: M=Manning, DW=Darcy-Weisbach, O&H=Oderkamp and Hedman, SB-sb=sandbed, silt-bank, SB-SB=sandbed, sand-bank.

Two factors that affect the range of resulting discharge values are: 1) bed sediment size effects and 2) differences in estimating the friction factor for the micro-approach. Osterkamp and Hedman [29] observed in perennial alluvial streams that the largest discharges occur in fine-grained bed material and decrease as the sandiness of the channel material increases; this trend is reversed once the median particle size exceeds 2 mm due to armoring. Formulations for the friction factor based on empirical data provide a more realistic approximation of frictional dissipation factors in natural rivers and tend to yield higher friction factor values than purely theoretical equations. The net effect of these more realistic, higher friction factors is lower computed discharge values.

Discussion The hydrologic models must account for the lower gravitational acceleration on Mars. Gravity scaling of the micro-approach is rather straightforward [see e.g., 30]. However, gravity is not an explicit term in the empirical macro-approach, and the lower Martian gravity should allow channels of given dimensions and meander wavelength to form at a slightly lower discharge than they would on Earth, with the exact value of the scaling coefficients varying with channel dimensions. The uncorrected macro-approach would overestimate the discharge values by about 50% [31]. Given the variability of paleodischarge values obtained from the individual methods applied to the cemented CMF paleochannels, it is like-

ly that the resultant envelope of values still incorporates the actual paleodischarge value.

Distinguishing induration agent for inferred Martian inverted channels has important implications for reconstructing the fluvial history. For example, lavas flowing into a valley can fill the original fluvial channel as well as the larger valley, resulting in the potential for an overestimation of channel width. On the basis of channel form alone, there is no diagnostic indicator of the indurating agent, but there are aspects of the preserved form that can suggest one mechanism was more likely than another. Noteworthy ridge attributes include: (1) the extent of network preservation, (2) the presence/absence of sedimentary structures, (3) the patterns of subsequent drainage, if developed, and (4) the pattern of inverted channel breakdown in response to weathering. These characteristics coupled with geologic setting regional context are important clues in assessing various indurating agents for Martian sinuous ridges.

Further study of inverted fluvial systems on Earth will help to elucidate the magnitude and relative timing of fluvial activity as well as the necessary climatic conditions on Mars.

Acknowledgements: The author is grateful to many individuals who have contributed to this research: T. Chidsey, D. Eby, R. Irwin, and J. Zimbleman for assistance in conducting field work and analysis; M. Osterloo for sharing the chloride database; and D. Burr, K. Edgett, A. Howard, and M. Malin for thought-provoking discussions.

References: [1] Williams R. M. E. and Edgett K. S. (2005) *LPSC XXXVI*, Abstract #1099. [2] Carr M. (1995) *JGR*, 100, 7479-7507. [3] Carr M. (1996) *Water on Mars*, Oxford U Press, 229 pp. [4] Howard, A. D. (1981) *Reports of the Planetary Geology Program, NASA TM 84211*, 286-288. [5] Williams R.M.E. (2007) *LPSC XXXVIII*, Abstract #1821. [6] Mangold N. et al. (2004) *Science*, 305, 78-81. [7] Kargel J. S. and Strom R. G. (1992) *Geology*, 20, 3-7. [8] Ruff S. W. and Greeley R. (1990) *LPSC XXI*, p. 1047-1048. [9] Hiesinger H. and Head J. W. (2002) *Planet. Space Sci.* p. 939-981. [10] Banks M. E. et al. (2008, submitted) *JGR*. [11] Burr (2008, submitted) *Icarus*. [12] Nussbaumer J. (2003) *6th Mars*, 3018. [13] Osterloo, et al. (2008) *Science*, 319, 1651-1654. [14] Scott D. H. and Tanaka K. L. (1986) *USGS Misc. Invest. Map, I-1802-A*. [15] Greeley R. and Guest J. E. (1987) *USGS Misc. Invest. Map, I-1802-B*. [16] Tanaka K. L. (1986) *JGR*, 91, E139-E158. [17] Hynek B. M. et al. (2008) *LPSC XXXIX*, Abstract #2353. [18] Hynek B. M. and Phillips R. J. (2001) *Geology*, 29, 407-410. [19] Zimbleman J. R. et al. (2003) *LPSC XXXIV*, Abstract #1390. [20] Hamblin W. K. (2004) *Beyond the visible landscape—Aerial Panoramas of Utah's Geology*, Regal Printing, 300 pp. [21] Harris D. R. (1980) *Brigham Young U Geo. Studies*, v. 27, p. 51-66. [22] Lorenz J. C. et al. (2006) *AAPG Bull.*, v. 90, p. 1293-1308. [23] Nuccio V. F. and Condon S. M. (1996) *USGS Bull.* 2000-O, 41 pp. [24] Nuccio V. F. and Robert S. M. (2003) *USGS Digital Data Series DDS-69B*, 39 pp. [25] Williams R.M.E. et al. (2007) *Central Utah – Diverse Geology of a Dynamic Landscape*, p. 221-235. [26] Williams R.M.E. et al. (2008 submitted) *Geomorphology*. [27] Jopling (1996) [28] Langbein W. B. and Leopold L. B. (1964) *Am. J. Science*, 262, p. 782-794. [29] Osterkamp, W. R. and Hedman E. R. (1982) *USGS Prof. Pap. 1242*, 37 pp. [30] Komar P. D. (1979) *Icarus* v. 37, p. 156-181. [31] Irwin R. P. et al. (2008, in press) *River confluences and the fluvial network*, John Wiley.